

Evaluation by Vickers indentation of fracture toughness of a phosphate biodegradable glass

J. CLÉMENT, P. TORRES, F. J. GIL, J. A. PLANELL

Dpt Ciència dels Materials i Enginyeria Metallúrgica, ETSEIB, Universitat Politècnica de Catalunya, Diagonal 647, 08028-Barcelona, Spain

R. TERRADAS, S. MARTINEZ

Dpt Cristallografia, Mineralogia i Recursos Minerals, Universitat de Barcelona, Martí i Franques s/n. 08028-Barcelona, Spain

Indentation tests are commonly used for the evaluation of fracture toughness of brittle materials, particularly glasses and ceramics, because this technique requires only a small polished area on the specimen surface from which a large number of data points can be generated rapidly. However, a wide variety of equations for the calculation of fracture toughness of ceramic materials by means of Vickers indentation are available. Such equations are obtained phenomenologically and their parameters adjusted in such a way that the K_{IC} values obtained are in good agreement with those obtained by conventional methods. This is the reason why it is necessary to check which type of equation reproduces more accurately the results obtained by means of conventional methods for the material which is going to be investigated. In the present work seven different fracture toughness equations widely used in glass and ceramic studies are considered and the results are compared with those obtained by conventional methods, such as single-edge notch beam (SENB) specimens tested in three-point bending. The role played by the applied indentation load is considered.

© 1999 Kluwer Academic Publishers

1. Introduction

The use of ceramic materials is of great interest for the repair and reconstruction of diseased or damaged parts of the musculoskeletal system. Ceramics used for this purpose are termed bioceramics [1]. In the last decades, physicochemical studies related with the dissolution mechanisms of glasses in water, lead to the development of glasses within a compositional interval which favors the gradual lixiviation of their constituents [2]. These glasses are formulated in the system ($\text{Na}_2\text{O}-\text{CaO}-\text{P}_2\text{O}_5$), where the network former is P_2O_5 , and they are made by melting together oxide forms of phosphorous, calcium and sodium in a platinum crucible at temperatures between 1000–1200 °C. The chemical composition of these glasses can be adjusted so as to obtain dissolution times ranging between a few days to several months. The first studies aiming to biomedical applications of such glasses were carried out with a molar content in P_2O_5 from 30 to 50% [3, 4]. Cytotoxicity tests, as well as *in vivo* implantation [4], revealed that such glasses are soluble in aqueous media and biocompatible with a very low cytotoxicity in hard and soft tissues. On complete dissolution the glasses leave no residues.

Given the structural function that a bone substitute should perform in service, the mechanical properties are always taken into account, and particularly the fracture toughness, K_{IC} , the reported values never being much

higher than $1 \text{ MPa m}^{1/2}$ [5]. In ceramic materials, the use of the Vickers indentation test for the evaluation of the fracture toughness has become widespread because of the simplicity of the specimen preparation, requiring only the provision of a small polished and reflective plane surface from which a large quantity of data points can be generated rapidly. However, the revision of the literature on the indentation K_{IC} testing of ceramic materials reveals a wide variety of phenomenological equations available. Besides, the morphology of the crack system that is formed during an indentation test is often complex and difficult to define clearly. Nevertheless, most of these models assume that either an idealized radial–median or a Palmqvist crack system is formed during a Vickers indentation test, from which the discrepancy between the indentation fracture toughness of a material and the fracture toughness as measured by conventional methods, such as SENB test, has often been reported [6].

The present work compares the K_{IC} results obtained using seven different models of indentation fracture toughness [7–13] with those obtained with SENB specimens tested in three-point bending. The influence of the applied indentation load is analyzed. The morphology of the indentation cracking is also evaluated by scanning electron microscopy (SEM).

2. Materials and methods

In this study the mechanical properties of a phosphate biodegradable glass in the system $\text{Na}_2\text{O}-\text{CaO}-\text{P}_2\text{O}_5$, named BV11, and with a molar content of CaO 44.5%, Na_2O 11.0% and P_2O_5 44.5%, were evaluated. The raw materials used for the elaboration of the material were $\text{NH}_4\text{H}_2\text{PO}_4$, Na_2CO_3 and CaCO_3 . The glass was obtained by melting together the different oxides on a platinum crucible at a temperature of 1200 °C followed by quenching on a metallic plate preheated at 500 °C. The material was finally annealed during 30 min at a temperature of 445 °C, corresponding to its glass transition temperature, and kept in a desiccator prior to use so as to limit the degrading effect of the environment on its surface.

In order to carry out the Vickers indentations, five specimens of BV11 were embedded in a polyester resin at room temperature and polished by means of 0.05 μm diameter alumina particles. Vickers indents on each specimen were introduced using a microhardness testing machine, with indentation loads of respectively 500, 300, 100, 50 and 25 g applied during 30 s. The indented surfaces were observed with an optical microscope in polarized light, in order to reveal stress birefringence. In Fig. 1, we represent a schematic of the Vickers indentation crack geometry.

The indentation fracture toughness of the material was evaluated selecting seven models commonly used in glass studies; models 1, 2, 3 and 4 consider that the emanating indentation cracks are radial-median type, model 5 corresponds to a Palmqvist crack system, and finally models 6 and 7 are formulations adjusting any kind of indentation crack system. In Fig. 2, we show the comparison of a radial median and a Palmqvist crack system around a Vickers indentation [12].

These models are presented in Table I, where P corresponds to the applied load of indentation (N), c the crack length (mm), a the indent length (mm) (see Fig. 1), H_v the Vickers hardness (GPa) and E the Young's modulus of the material (GPa). The ratio of hardness to modulus H/E was evaluated in a previous work [14] by measurements of the elastic recovery at hardness indentations, observing the relative contraction of the surface diagonals of a Knoop impression. The analysis gives [15]

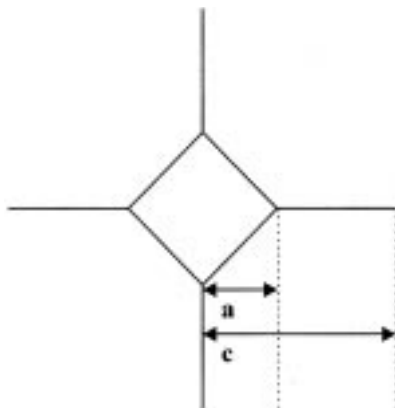


Figure 1 Illustration of the indentation crack geometry.

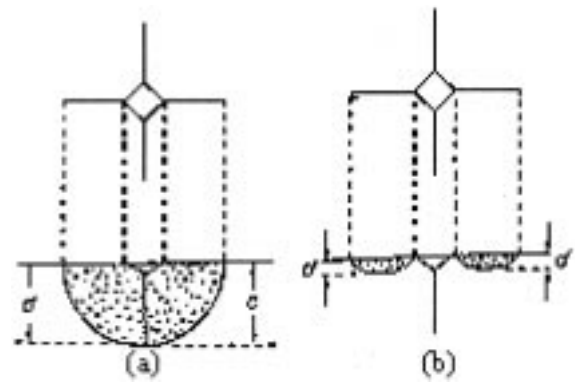


Figure 2 Comparison of median (a) and Palmqvist (b) cracks around a Vickers indentation.

$$\frac{b'}{a'} = \frac{b}{a} - \alpha \frac{H}{E} \quad (1)$$

where $b/a = 1/7$ is the nominal ratio of short to long half-diagonal, b'/a' is the corresponding value of the recovery, and α is a dimensionless constant.

For the analysis of the indentation crack morphology and the evaluation of the mechanical properties of the glasses by three-point bending test, beam specimens of $4 \times 3 \times 25$ mm were cut with a diamond disc and polished by means of 0.05 μm diameter alumina particles. The specimens were then annealed at 445 °C during 30 min to eliminate the residual stresses that may have appeared during cutting and polishing.

In order to observe the indentation crack pattern by electron microscopy, a single indentation was made in the center of the surface of 10 specimens with loads of, respectively, 500, 300, 100, 50 and 25 g during 30 s, hence being two samples indented with the same load. Then, the specimens were fractured by three-point bending, in such a way that the indented face was stressed in traction.

For the measurement of the fracture toughness by conventional three-point bending test, eight samples were notched in such a way that $a/W \approx 0.5$ and K_{IC} was evaluated according to

$$K_{IC} = YSa^{\frac{1}{2}} \quad (2)$$

with $S = (3PL)/(2BW^2)$ [16]. P corresponds to the breakload (N), and

$$Y = 1.99 - 2.47\left(\frac{a}{W}\right) + 12.97\left(\frac{a}{W}\right)^2 - 23.17\left(\frac{a}{W}\right)^3 + 24.8\left(\frac{a}{W}\right)^4$$

All the three-point bending tests were performed in an electromechanic testing machine equipped with a 10 kN capacity load cell, using a support span of 20 mm, and working at a cross-head speed of 0.2 mm min^{-1} . A scanning electron microscope (SEM) was used for the fractographic study of the indentation cracking. All the specimens were kept at all times inside a desiccator and only exposed to the environment during the tests.

3. Results and discussion

The fracture toughness of BV11, calculated with SENB specimens tested in three-point bending, showed average

TABLE I Selected equations for K_{IC} measurements with Vicker's indentations

No	Ref.	Radial–Median type crack system	Palmqvist type crack system
1	[7]	$0.0154(E/H_v)^{1/2}(P/c^{3/2})$	
2	[8]	$0.0095(E/H_v)^{2/3}(P/c^{3/2})$	
3	[9]	$0.028(H_v a^{1/2})(E/H_v)^{1/2}(c/a)^{-1.5}$	
4	[10]	$0.0303(H_v a^{1/2})(E/H_v)^{2/5} \log(8.4 a/c)$	
5	[11]		$0.015(E/H_v)^{2/3}(P/c^{3/2})(c/a - 1)^{-1/2}$
6	[12]		$0.0495(H_v a^{1/2})(E/H_v)^{2/5}(c/a)((c/18a) - 1.51)$
7	[13]		$0.0782(H_v a^{1/2})(E/H_v)^{2/5}(c/a)^{-1.56}$

values of $0.65 \pm 0.08 \text{ MPa m}^{1/2}$. The results of the indentation fracture toughness calculated with the different models for each applied indentation load are shown in Table II. In this table, the gray zones correspond to the K_{IC} values suitable with the results obtained in three-point bending. Fig. 3 compares the ranges of fracture toughness values calculated with each formula with that obtained in three-point bending test using SENB specimens. This figure also shows the influence of the applied indentation load on the values of the fracture toughness evaluated with the different models.

It can be noticed from Figure 3 and Table II that, whatever the indentation load applied, the indentation fracture toughness equations of Anstis (formula 1) [7], Laugier (formula 2) [8], and Lawn (formula 3) [9], both corresponding to a radial–median crack system, show values of K_{IC} smaller than those obtained in the three-point bending test. However, the formula of Blendell (formula 4) [10], also corresponding to a radial–median crack system, gave values of fracture toughness quite similar to that of SENB specimens, presenting the best values for indentation loads of 500, 300 and 100 g. For lower indentation loads, the values of K_{IC} seemed to decrease, although remaining in the same order of magnitude. The two general equations of Liang (formula 6) [12], and Lankford (formula 7) [13], developed for any kind of crack system, also presented values of fracture toughness similar to that obtained in three-point bending for each indentation load. Finally, The equation of Laugier (formula 5) [11], corresponding to a Palmqvist crack system, showed increasing values as the indentation load decreased, obtaining finally results in the same range than in the three-point bending tests for loads of 100, 50 and 25 g.

These results can be interpreted with the microscopic

analysis of the indentation cracking. Fig. 4 shows micrographs of the fractured surface of BV11 specimens in the zone of the indentation. In these micrographs, the morphology of the indentation cracking and its evolution with the applied indentation load can be observed. In Fig. 4a and b, corresponding, respectively, to indentation loads of 500 and 300 g, it can be clearly noticed the typical morphology of a radial–median crack system, with the presence of a circular crack emanating from the base of the plastic deformation zone which evolves into a half-penny crack during the contact cycle. In these two micrographs the formation of lateral cracks beneath the deformation zone, running parallel to the surface can also be appreciated. This crack system appears during the unloading of the indenter. Lateral cracks are usually regarded as a secondary indentation crack system which does not control strength, and which is difficult to model [17]. These observations explain the reason why, at high indentation loads, the equation of Blendell (formula 4) [10], corresponding to a median crack system, shows K_{IC} results quite similar to those obtained with SENB specimens. However, in Table II It can be noticed that the formulae 1, 2 and 3, also corresponding to a median crack system, showed smaller values of K_{IC} than the Blendell equation. This observation shows that, although the morphology of the indentation cracking is perfectly defined, all the approximation equations corresponding to this crack system are not suitable and the choice of the formula depends also on the material tested.

In the micrograph (Fig. 4c) corresponding to an indentation load of 100 g, it can be observed that the typical half-penny shape of a median crack system does not appear as clearly as in the micrographs of Fig. 4a and b. Indeed, the circular cracks emanating

TABLE II Results of the fracture toughness values of BV11 evaluated with the different equations for each applied indentation load. The gray zones indicate the values suitable with the results obtained by three-point bending tests

Formula	Indentation load (g)				
	500	300	100	50	25
1	0.39 ± 0.02	0.44 ± 0.04	0.48 ± 0.03	0.45 ± 0.03	0.46 ± 0.03
2	0.41 ± 0.02	0.47 ± 0.04	0.51 ± 0.03	0.47 ± 0.04	0.49 ± 0.02
3	0.33 ± 0.02	0.38 ± 0.03	0.41 ± 0.03	0.38 ± 0.03	0.39 ± 0.03
4	0.67 ± 0.03	0.71 ± 0.04	0.68 ± 0.02	0.61 ± 0.02	0.55 ± 0.02
5	0.36 ± 0.03	0.47 ± 0.06	0.62 ± 0.06	0.60 ± 0.07	0.72 ± 0.10
6	0.56 ± 0.02	0.59 ± 0.04	0.60 ± 0.03	0.55 ± 0.03	0.53 ± 0.03
7	0.62 ± 0.04	0.71 ± 0.06	0.79 ± 0.05	0.74 ± 0.05	0.75 ± 0.06

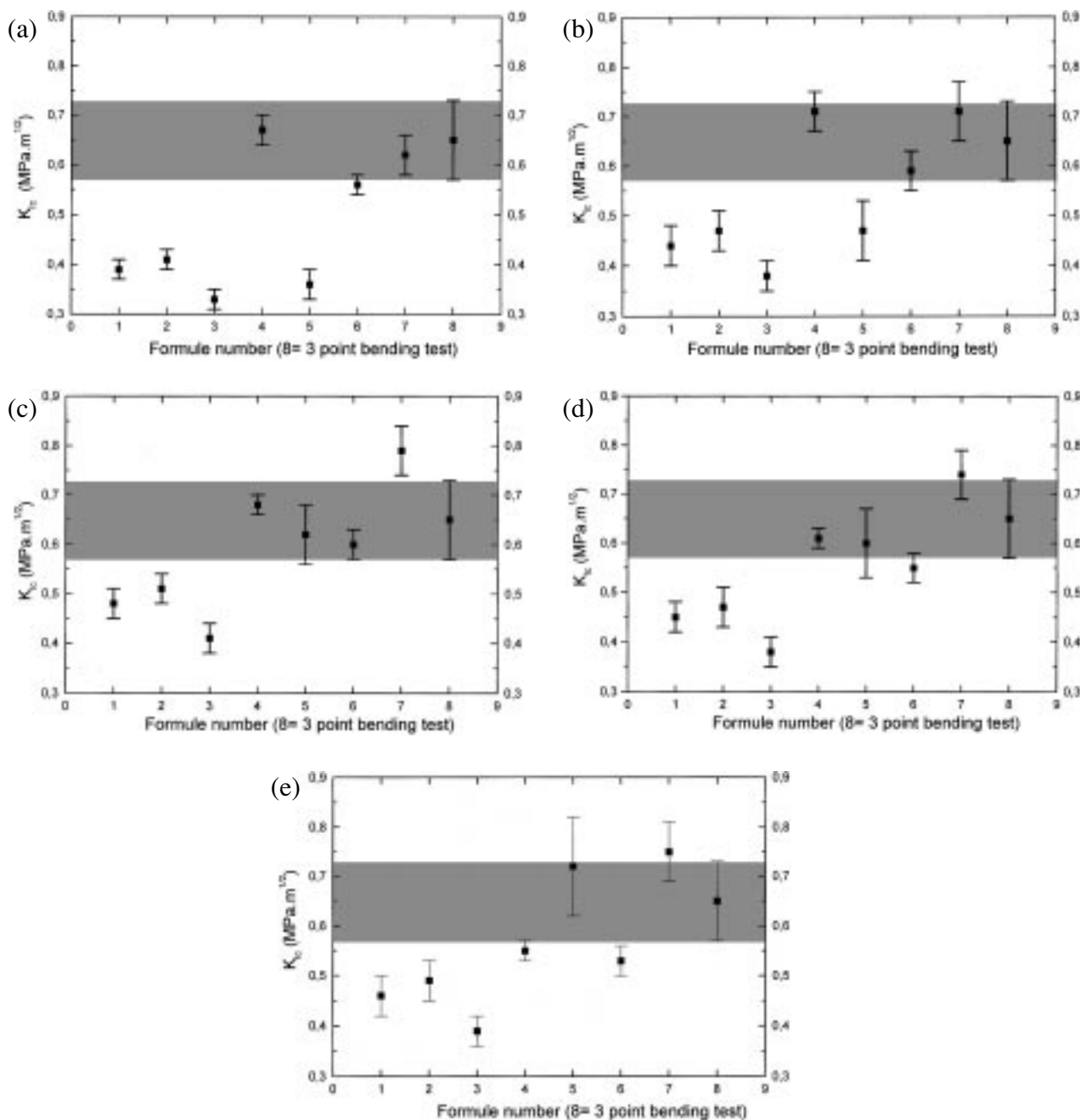


Figure 3 Comparison of the K_{IC} values obtained with the different formulations with that obtained in three-point bending tests. Indentation load: (a) 500 g, 30 s; (b) 300 g, 30 s; (c) 100 g, 30 s; (d) 50 g, 30 s; (e) 25 g, 30 s.

from the plastic deformation zone seem not to have sufficient energy to join together. This morphology appears to be a transition between the idealized median and Palmqvist indentation crack systems. In the micrograph (Fig. 4d) corresponding to a load of 25 g, the same type of morphology can be observed.

These observations explain clearly why the values of K_{IC} obtained with median crack system equations, such as formulae 1, 2, 3 and 4, decrease as the indentation load decreases, and the formula 5, corresponding to a Palmqvist crack system, show increasing values as the indentation load decreases. These observations show the great importance of the applied indentation load on the morphology of the indentation cracking, and consequently on the choice of the indentation fracture toughness equation.

4. Conclusions

In this work, the fracture toughness of a biodegradable phosphate glass has been determined by means of Vickers indentation and three-point bending tests. The results showed values of $0.65 \pm 0.08 \text{ MPa m}^{1/2}$, which are quite suitable for a bone bonding material.

The comparison of the indentation fracture toughness results, calculated with seven selected equations, with that obtained with conventional three-point bending tests of SENB specimens showed the importance of the applied indentation load on the similarity of the values obtained. Indeed, the indentation load showed to have a clear influence on the indentation cracking system, developing radial–median crack system for high and medium loads, and tending to Palmqvist crack system for lower loads.

Moreover, this study revealed that, although the

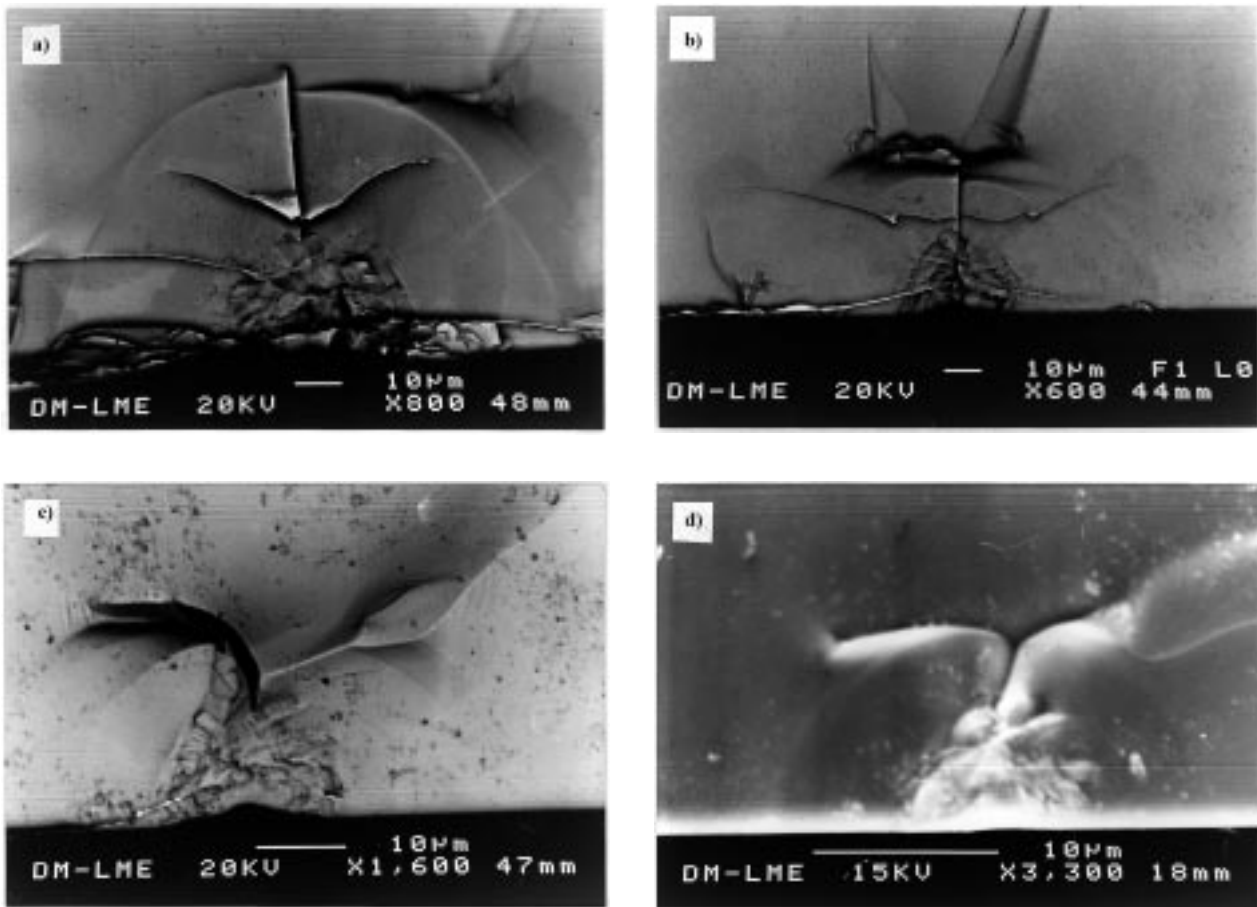


Figure 4 Micrographs of the indentation cracking. Indentation load: (a) 500 g, 30 s; (b) 300 g, 30 s; (c) 100 g, 30 s; (d) 25 g, 30 s.

morphology of the indentation cracking is perfectly defined for any material at any indentation conditions, the choice of the best adjusting model for the K_{IC} determination is difficult and it always needs a comparison with the results obtained by conventional tests, since the values obtained are strongly dependent on the chosen model.

This study also revealed that, although all specimens were kept in a dessicator before testing, the degrading effect of the environment humidity on the surface of the glass should be taken into account as, for high indentation loads, chipping of the surface could be observed after completion of the contact. In order to avoid this phenomenon, indentation tests should be carried out in an inert atmosphere for further studies.

To conclude, it appeared that for a biodegradable phosphate glass, indentation loads of 300 g applied during 30 s using the approximation of Blendell [10] show values quite similar to those obtained with SENB specimens tested in three-point bending.

Acknowledgment

The authors are grateful to the CICYT for providing financial support through the project MAT96-0981 and the European Commission for the concession of the Marie Curie Research Training Grant through the contract n°ERBFMBICT972152.

References

1. L. L. HENCH, *J. Amer. Ceram. Soc.* **74** (1991) 1487.

2. C. F. DRAKE and M. GRAHAM, "Inorganic glasses as slow release herbicides and fungicides", (Chemical Society, London, 1976).
3. J. BURNIE, T. GILCHRIST, S. R. I. DUFF, C. F. DRAKE, N. G. L. HARDING and A. J. MALCOLM, *Biomaterials* **2** (1981) 244.
4. J. BURNIE and T. GILCHRIST, in "Ceramics in surgery", edited by P. Vicenzini (Elsevier, the Netherlands, 1983) p. 169.
5. J. A. PLANELL, M. VALLET-REGÍ, E. FERNANDEZ, L. M. RODRIGUEZ, A. SALINAS, O. BERMÚDEZ, B. BARADUC, F. J. GIL and F. C. M. DRIESSENS, *Bioceramics* **7** (1994) 17.
6. C. B. PONTON and R. D. RAWLINGS, *Mater. Sci. Technol.* **5** (1989) 865.
7. G. ANSTIS, P. CHANTIKUL, B. LAWN and D. MARSHALL, *J. Amer. Ceram. Soc.* **64** (1981) 533.
8. M. LAUGIER, *J. Mater. Sci. Lett.* **4** (1985) 1539.
9. B. R. LAWN, A. G. EVANS and D. B. MARSHALL, *ibid.* **63** (1980) 574.
10. J. BLENDPELL, PhD Thesis, Massachusetts Institute of Technology, Cambridge, MA, (1979).
11. M. LAUGIER, *J. Mater. Sci. Lett.* **6** (1987) 355.
12. K. M. LIANG, G. ORANGE and G. FANTOZZI, *J. Mater. Sci.* **25** (1990) 207.
13. J. LANKFORD, *J. Mater. Sci. Lett.* **1** (1982) 493.
14. F. J. GIL, R. TERRADAS, J. CLEMENT, G. AVILA, S. MARTINEZ and J. A. PLANELL, *Bioceramics* **10** (1997) 553.
15. D. B. MARSHALL and B. R. LAWN, Microindentation techniques in materials science and engineering, ASTM special technical publication 889, International Metallographic Society (1984) 26-45.
16. Department of Defense, United States of America (1983) MIL-STD-1942(MR).
17. R. F. COOK and G. M. PHARR, *J. Am. Ceram. Soc.* **73** (1990) 787.

Received 9 February
and accepted 3 August 1998